第 32 卷第 7 期
2016 年 7 月

无 机 化 学 学 报
CHINESE JOURNAL OF INORGANIC CHEMISTRY

Vol.32 No.7
1127-1134

反应器内流场分布对球形氢氧化镍生长结晶的影响

唐俊杰 刘 燕* 田 磊 王东兴 张廷安
(东北大学多金属共生矿生态化冶金教育部重点实验室,沈阳 110819)

摘要:在相同停留时间、不同搅拌桨线速度条件下,利用化学沉淀法制备球形氢氧化镍样品并运用 SEM 技术考察制得样品的形貌。研究表明:在相同的停留时间和化学条件下,随着搅拌桨线速度的提高样品的微观形貌由无定型状晶体变为大颗粒类球状晶体再变为较规则的球状晶体。利用 PIV 物理模拟技术模拟反应器内流场分布情况并结合 XRD 表征结果分析得出:在相同的停留时间和化学条件下,反应器内流场分布越均匀、速度矢量越大氢氧化镍晶体的生长越完整,结晶性、球形度和相对结晶度越高,并从流场分布的角度描述了球形氢氧化镍生长结晶的过程。

关键词:球形氢氧化镍;流场分布;相对结晶度;生长结晶
中图分类号:O614.81+3 **文献标识码**:A **文章编号**:1001-4861(2016)07-1127-08
DOI:10.11862/CJIC.2016.156

Influence of Flow Field Distribution on the Crystallization of Spherical Nickel Hydroxide in Reactor

TANG Jun-Jie LIU Yan* TIAN Lei WANG Dong-Xing ZHANG Ting-An
(*Key Laboratory for Ecological Utilization of Multimetallic Mineral, Ministry of Education, Northeastern University, Shenyang* 110819, *China*)

Abstract: The spherical nickel hydroxide was synthesized by chemical precipitation method under the conditions of the same stay time but different linear velocities of the stirring blades. Then the morphologies of the spherical $Ni(OH)_2$ were characterized by SEM. In the same retention time and chemical condition, it was found that with increasing the linear velocity, the morphology of the spherical $Ni(OH)_2$ changed from amorphous crystals to large near spherical particles at first, and then to regular spherical crystals finally. The flow field distribution in the reactor was simulated by PIV physical model technology. And XRD results show that in the same retention time and chemical condition, more uniform flow field distribution in the reactor and higher velocity vector can lead to more complete $Ni(OH)_2$ crystals, higher relative crystallinity and higher degree of sphericity. Moreover, the crystallization process of spherical $Ni(OH)_2$ was described from the flow field viewpoint.

Keywords: spherical $Ni(OH)_2$; flow field distribution; relative crystallinity; crystallization

0 Introduction

Spherical $Ni(OH)_2$ is one of the most important battery materials which has been widely applied in communication, spaceflight, digital and so on. Some problems such as large structure differences in different batches always appear in the manufacture of spherical $Ni(OH)_2$ products. Peng et al. studied the influence of turbine blade and propelled paddle on the crystallization of spherical $Ni(OH)_2$, and they concluded that in

收稿日期:2016-01-25。收修改稿日期:2016-05-29。
国家国家自然科学基金云南联合重点基金(No.U1402271,U1202274)资助项目。
*通信联系人。E-mail:573080224@qq.com

the same energy consumption, the use of turbine blade can get more uniform growth product[1-3]. Shen et al. explained the growth process of spherical $Ni(OH)_2$ crystal by a growth model[4-5]. Al-Hajry et al. studied the growth of flower-shaped Ni $(OH)_2$ crystal, and they suggested that the flower-shaped crystal is consisted of thin nanosheets which are connected each other and they form network-like morphologies[6]. Hironori et al. studied the crystal growth of β-$Ni(OH)_2$ in hydrothermal synthesis process, and the changes of the number and size of crystals with the hydrothermal reaction period were quantitatively analyzed by using the TEM images. Moreover, the crystallization was controlled by the size limit of the nanochannels[7].

The stirring plays a key role in the control of the crystallization process. Sancho et al. studied the characteristics of the mixing layer flow in a cylindrical reactor by PIV and PLIF technology, and they concluded that the rapid irreversible reaction particles with smaller displacement in the flow field cannot significantly increase the reaction rate, but it can improve the mixing degree of the reactants[8-13]. Fukushima et al. used the PIV and PTV technique to investigate the particle dispersion in different regions of the reactor during the mixing process, and get relevant experience for controlling the crystallization which is related to concentration[14-15].

The control of the spherical $Ni(OH)_2$ crystallization has great relationship to the concentration of the material in the reactor and the degree of mixing. To investigate the process of the spherical $Ni(OH)_2$ crystallization, scientists mainly take the temperature, pH value (ammonia content), reactant supersaturation, mixing intensity and paddle type and other aspects into consideration at present. However, the influence of the field distribution inside reactor on the crystal growth of spherical Ni $(OH)_2$ was rarely studied. Therefore, in this study the spherical Ni $(OH)_2$ was synthesized by chemical precipitation method under different linear velocities of the stirring blades. The morphologies and relative crystallinity of the spherical Ni $(OH)_2$ were characterized by SEM and XRD. Then the flow field distribution in the reactor under different linear velocities of the stirring blades was simulated by PIV physical model technology. The relationship between flow flied distribution and Ni $(OH)_2$ crystallization was concluded from the experimental and simulation results. This study provides a theoretical basis and experience, both for reducing the structure difference in $Ni(OH)_2$ industrial products and the structure design of industrial reactor.

1 Experimental

1.1 Reactor design

According to the investigation on the spherical $Ni(OH)_2$ industrial production reactor, and the understanding of the hydrodynamic conditions such as the velocity field, concentration field, temperature field and residence time distribution in the reactor and the transfer behavior, a 200 L organic glass model reactor was designed by $N_L=N_s(D_S/D_L)^X$ similar geometry principle (for this system the magnification factor X= 1~3/4, because the industrial chemical precipitation method for the preparation of spherical $Ni(OH)_2$ system is solid-liquid suspension system).

1.2 Preparation of spherical $Ni(OH)_2$

According to the industrial process of spherical $Ni(OH)_2$ preparation, the chemical precipitation method was applied to the preparation of spherical $Ni(OH)_2$ in this experiment. The reaction temperature of the system is controlled at 50~57 ℃, and the pH value is controlled at 11 ~11.7. A certain concentration of nickel sulfate solution, ammonia, sodium hydroxide solution in a certain proportion was filled to the bottom of the reactor. Under the same residence time, the sample is prepared under the stirring paddle line speed of 1, 3, 5 and 7 $m\cdot s^{-1}$, and then the sample is filtered and washed to dry, waiting for measurement.

1.3 SEM experiments

When the impeller line speed is 1 $m\cdot s^{-1}$ and 3 $m\cdot s^{-1}$, the $Ni(OH)_2$ particles are irregular shape crystals with different size, and the surface of the crystal is formed by the stacking of lamella micro-crystals with attached particles, such as Fig.1~2. When the impeller line speed is 5 $m\cdot s^{-1}$, $Ni(OH)_2$ particles formed many near spherical crystals, the surface of which is formed

by the accumulation of many well-defined lamellar micro-crystals, such as Fig.3. When the impeller line speed is 7 $m \cdot s^{-1}$, Nickel hydroxide particles formed spherical crystals with similar morphology and size, and the surface of these crystals is composed of the accumulation of many micro-crystals with clear stripes, such as Fig.4.

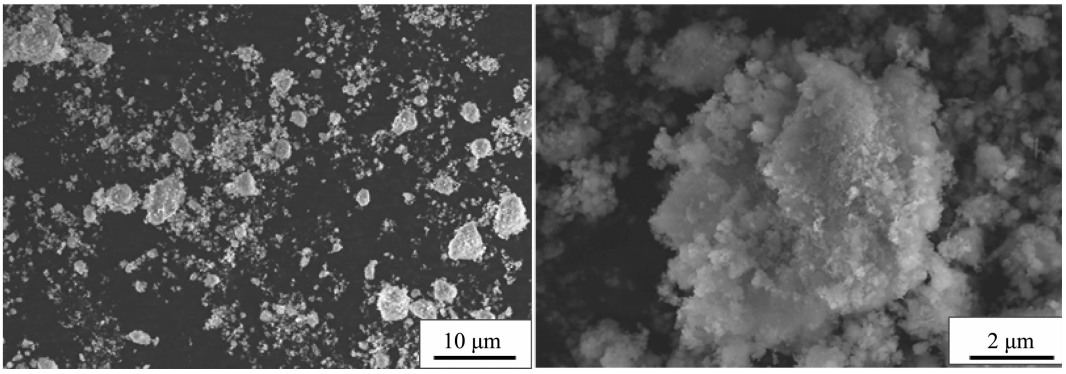

Fig.1　SEM image of $Ni(OH)_2$ particles (impeller line speed 1 $m \cdot s^{-1}$)

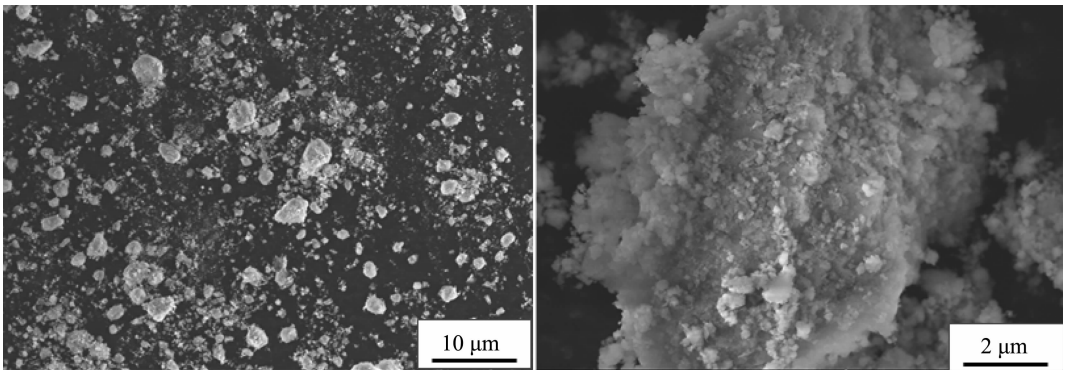

Fig.2　SEM image of $Ni(OH)_2$ particles (impeller line speed 3 $m \cdot s^{-1}$)

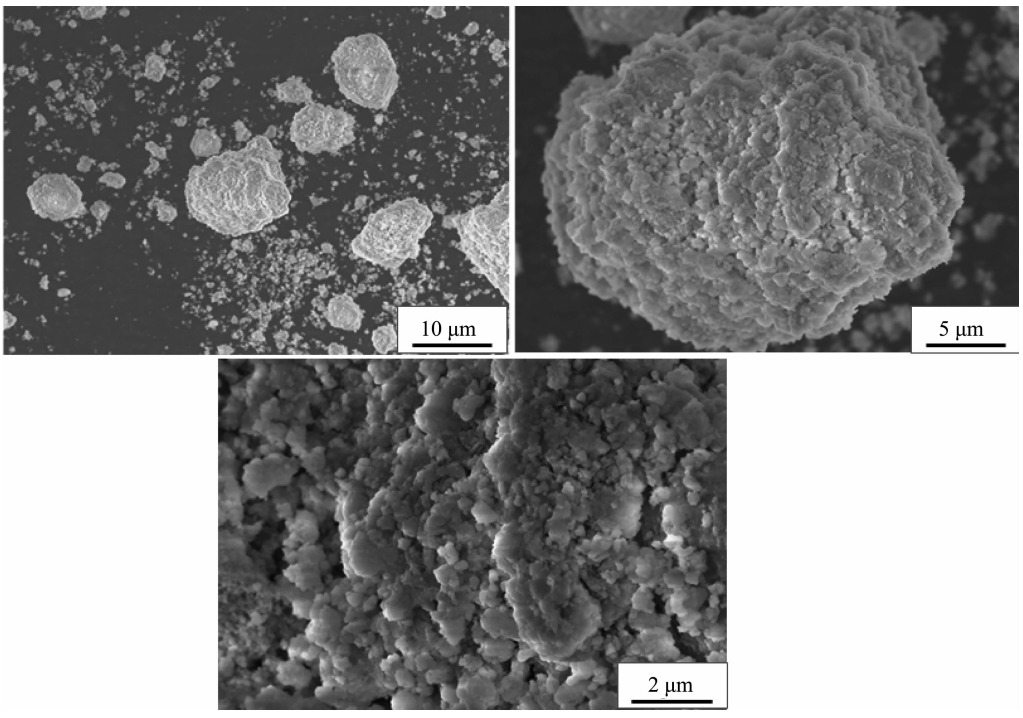

Fig.3　SEM image of $Ni(OH)_2$ particles (impeller line speed 5 $m \cdot s^{-1}$)

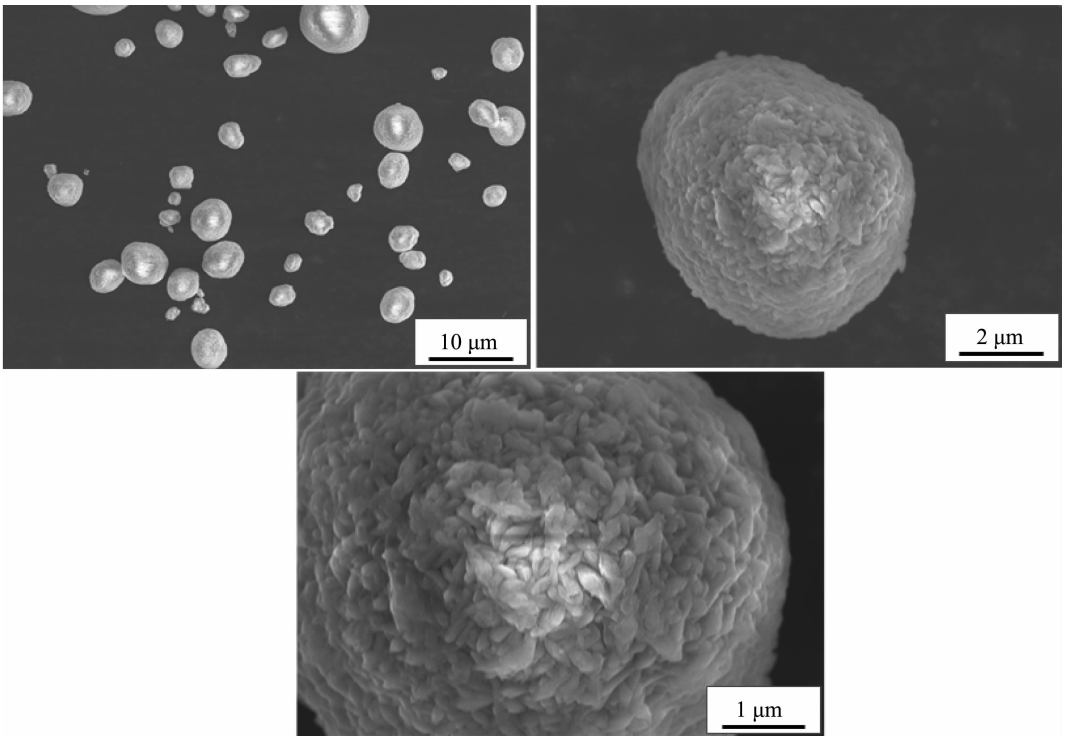

Fig.4 SEM image of $Ni(OH)_2$ particles (impeller line speed 7 $m \cdot s^{-1}$)

2 Results and discussion

2.1 PIV analysis

The crystallization porcess of spherical $Ni(OH)_2$ crystal can be divided into nucleation and crystal growth. Therefore, if the nucleus formation speed is fast and the crystal growth rate is slow, the nucleus will gradually form amorphous $Ni(OH)_2$ crystal. Ammonia is commonly used as a compounding agent which reacts with nickel ions to lower the concentration of reactants in industry, and the nucleation and growth rate of nickel hydroxide crystal can reach a reasonable reaction rates to form spherical nickel hydroxide (Equation **1**). The flow velocity vector and distribution in the reactor determine the mixed uniform rate and state of reagent and ingredient, which also indirectly affects the crystallization, spheri-city, growth uniformity of spherical $Ni(OH)_2$ and other important products indicators.

$$Ni^{2+}+6NH_3 \cdot 3H_2O=[Ni(NH_3)_6]^{2+}+6H_2O,$$
$$Ni^{2+}+2OH^-=Ni(OH)_2\downarrow \quad (1)$$

When the impeller line speed is 1 $m \cdot s^{-1}$, the cloud image of the absolute velocity vector in the reactor is shown in Fig.5. It can be seen from the graph that in both sides and the bottom area of the mixing paddle the velocity vector distribution is larger, which is the relatively high velocity zone of the liquid flow, and the direction of the liquid flow is from the bottom to the top. Three stirring circulation appeared in the reactor A, B and C areas, and the velocity vector in A, B and C areas is lower than other areas. When the impeller line speed is 3 $m \cdot s^{-1}$, the cloud image of the absolute velocity vector in the

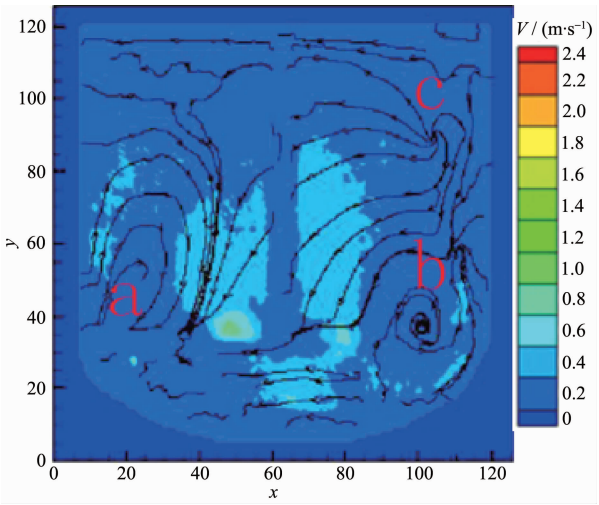

Fig.5 Cloud image of the system (absolute velocity vector 1 $m \cdot s^{-1}$)

reactor is shown in Fig.6. It can be seen from the graph that in both sides and the bottom area of the mixing paddle the velocity vector distribution is larger than before, but in the three circulation flow areas the velocity vector distributions show no significantly change. The area such as A, Band C is named as stirring dead zone. In the above two kinds of flow field distribution, because the velocity vector distribution in the reactor is low, the range of the stirring dead zone increases, which leads to the slowly mixing rate of the reaction materials and cooperation agent ammonia, and to low mixed degree of uniformity, consequently the $Ni(OH)_2$ crystal nucleation rate is fast but crystal growth rate is slow, forming amorphous crystalline with varying sizes (Fig.1~2).

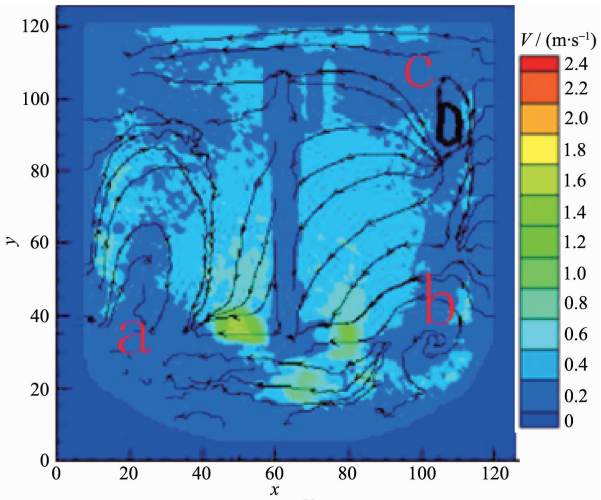

Fig.6　Cloud image of the system (absolute velocity vector 3 m·s^{-1})

As shown in Fig.7, when the impeller line speed increases to 5 m·s^{-1}, the fluid flow direction is from bottom to up, which is similar to that when the impeller line speed is 1 and 3 m·s^{-1}. The relatively high liquid flow velocity region at both sides of the shaft and the bottom of the stirring paddle expands and the velocity vector increases. At the A, B and C areas the stirring circulation velocity reactor show little variation with the increase of the stirring paddle line speed, but the mixing circulation range is reduced obviously. Due to increasing the flow velocity vector in the reactor and decreasing the stirring dead zone range, the mixed uniform extent of reactor reactant and cooperation agent raise, same to mixing rate. $Ni(OH)_2$ particles get together and grow into many large spherical crystals (Fig.7). Since in the reactor flow velocity vector and distribution uniform has not achieved ideal value, the aggregation growth of the spherical crystals does not aggregate, and not collide with each other and break to enter into the secondary crystallization stage, therefore does not form good sphericity of spherical nickel hydroxide crystal.

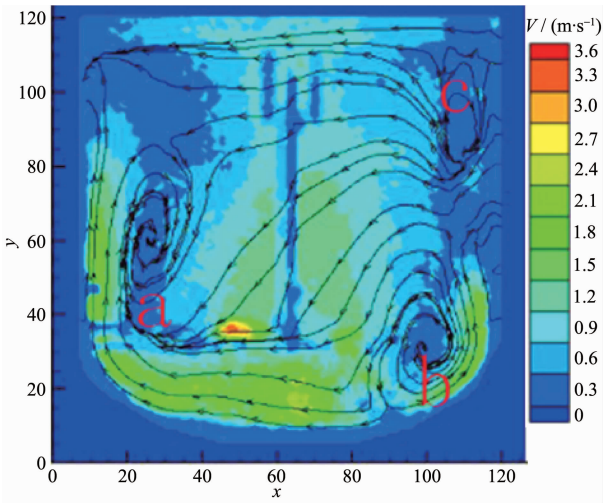

Fig.7　Cloud image of the system (absolute velocity vector 5 m·s^{-1})

As shown in Fig.8, when the impeller line speed increases to 7 m·s^{-1}, the relatively high liquid flow velocity region at both sides of the shaft and the bottom of the stirring paddle expands and the velocity vector continues to increase, and at the A, B and C

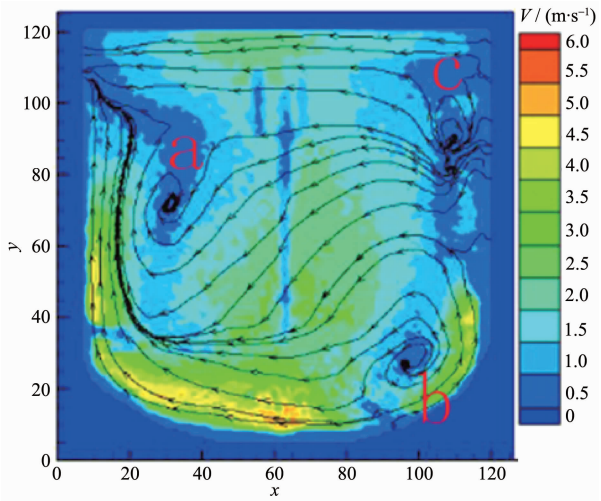

Fig.8　Cloud image of the system (absolute velocity vector 7 m·s^{-1})

areas the stirring circulation velocity reactor still doesn´t increase obviously, but the mixing circulation range gets smaller. Due to the change of the fluid flow distribution in the reactor, the mixed uniform extent of reactor reactant and mixing rate continue to rise. The nucleation rate and growth rate of the $Ni(OH)_2$ crystals reached a relative equilibrium, and under high speed flow field larger crystals formed many crystalline, sphericity, homogeneous volume spherical $Ni(OH)_2$ crystal by collision crushing secondary crystallization (Fig.8).

The agglomeration effect of particles plays a key role in the entire process of the crystal growth of spherical $Ni(OH)_2$[1]. When the impeller line speed is 1 or 3 $m \cdot s^{-1}$, the flow velocity vector is low and flow field distribution is not uniform in the reactor, which leads to the results that the mixed uniformity of the reactant is low, therefore, agglomeration rate of $Ni(OH)_2$ particles is low. So most of the nickel ion and ammonia ions does not occur the complexation reaction, but formed the nickel hydroxide precipitation. When the stirring paddle line speed increases to 5 $m \cdot s^{-1}$, the flow velocity vector becomes larger in the reactor, and the stirring circulation dead range is narrow, the flow field distribution is more uniform, so the mixed uniformity of the complexing agent and reactant improved, and more nickel ions complexation reacts with ammonia ions, which lead to slow rate of crystal nucleation, and to increasing crystal aggregation rate at the same time, particles agglomerate into many complete crystallization of large crystals with the same residence time. It can be concluded that as increasing flow velocity vector and uniform distribution in the reactor, the nickel hydroxide particles aggregation rate and sphericity also increases. When the stirring paddle line speed is 7 $m \cdot s^{-1}$, the distribution of flow field in the reactor and uniformity of velocity vector reach an ideal value, and the mixing of the complexing agent and the reactant reach an ideal state, and appropriate complexing reaction balance the crystal nucleation and crystal growth rate. At high speed flow field some large crystal aggregates collide and break to occur the secondary crystallization, and spherical nickel hydroxide crystals with uniform size and high degree form. It is shown that in the reactor only flow velocity vector reach a fixed value, large particles of $Ni(OH)_2$ crystal can lead to aggregation burst into the secondary crystallization, therefore, the crystal growth of uniformity is improved.

2.2 XRD analysis

The XRD instrument used in this experiment is D8 Advance X XBruker ray analyzer produced by German Bruker company. Light tube type is Cu target, ceramic X light tube. λ=0.154 06 nm, scan range is 10°~90°, the scanning speed is 2°·min^{-1}. XRD patterns of the samples which were prepared at different mixing speed is shown in Fig.9.

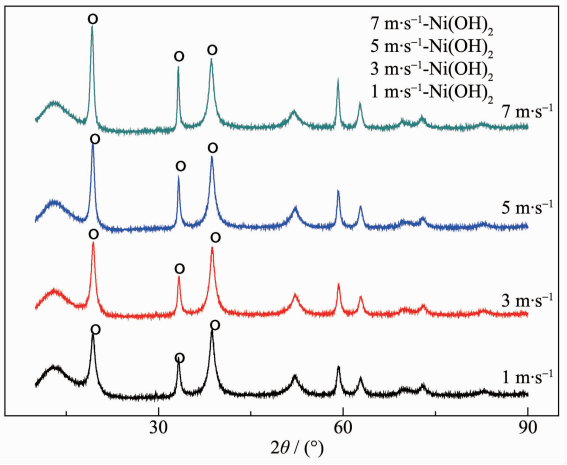

Fig.9 XRD patterns of the samples at different mixing speed

From Fig.9 it can be found that the main peak is nickel hydroxide, and other crystal items were not observed. When the line speed is 7 $m \cdot s^{-1}$, the diffraction peak in the XRD spectrum is highest, the half width of the peak is minimum, and the relative crystallinity of the best. If the best relative degree of crystallinity samples prepared at 7 $m \cdot s^{-1}$ is treated as relative crystallinity of 100%, according to amorphization formula $A=(1-U_0I_x/U_xI_0)\times100\%$, the calculation of amorphous salinity of each sample is plotted in a linear graph, as shown in Fig.10. Moreover, the relationship between line speed V ($m \cdot s^{-1}$) and amorphization: $A=1-0.479\ 4e^{0.104\ 1V}$ can be obtained according to Fig.10.

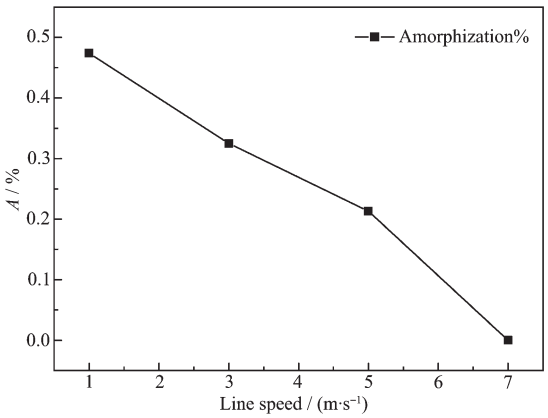

Fig.10　Relationship between line speed and amorphization

2.3　Relative particle size difference analysis

The particle size distribution instrument used in this experiment is MASTERSIZER 2000 produced by Malvern Instruments Ltd. The particle size distribution of the sample at different mixing speed is given in Table 1. From Table 1 it can be found that when the line speed is 7 m·s^{-1}, the relative particle size difference $F=d_{0.9}-d_{0.5}$ is minimum. Moreover, according Table 1 can be obtained Fig.11. From Fig.11 can lead to the relationship between relative particle size difference and line speed: $F_{(0.5\text{-}0.9)}=-15.59\ln V+41.172$.

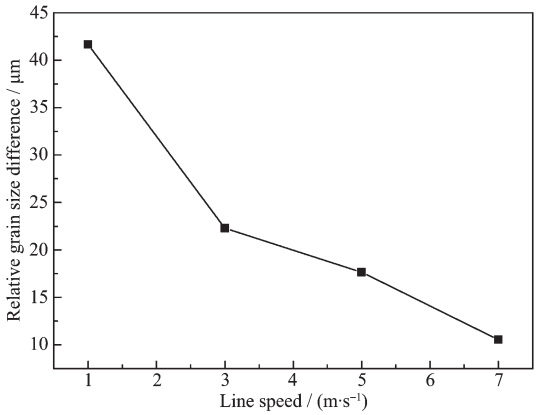

Fig.11　Relative particle size difference at different mixing speed

Table 1　Particle size distribution and size difference

Line speed / (m·s^{-1})	1	3	5	7
$d_{0.5}$ / μm	8.406	4.505	4.777	11.214
$d_{0.9}$ / μm	50.076	26.781	22.425	21.747
$(d_{0.9}-d_{0.5})$ / μm	41.670	22.276	17.648	10.533

2.4　CV analysis

The electrochemical activity is the basic indicator of $Ni(OH)_2$. The $Ni(OH)_2$ samples prepared of different stirring line speeds are compressed with carbon black and adhesive in proportion as 7:2:1 into sheets electrode. CV Scan is tested at the speed of 10 mA·s^{-1} in the range of 0~0.6 V, while the Hg/HgO is selected as the contrast electrode. The cycle voltammogram is shown in Fig.12. When the line speed is 7 m·s^{-1}, the area of electrochemical activity and peak current reach the maximum, which show the best electrochemical performance.

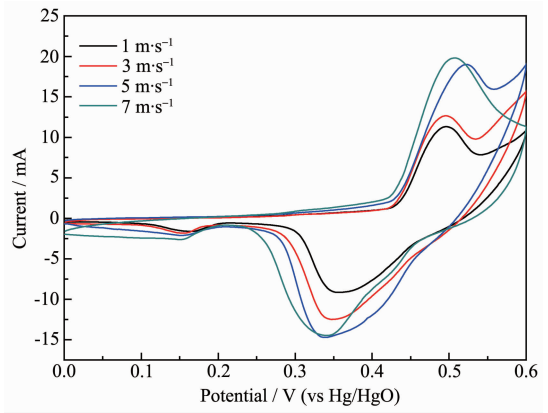

Fig.12　CV curves of $Ni(OH)_2$ samples at different mixing speed

3　Conclusions

(1) In the same retention time and chemical condition, the growth integrity, uniform, crystallization, sphericity and the particles aggregation rate of spherical $Ni(OH)_2$ crystals is proportional to the distribution range of the flow velocity vector and uniformity in the reactor.

(2) In the same retention time and chemical condition, large particles of $Ni(OH)_2$ crystals can lead to aggregation burst and the secondary crystallization to form $Ni(OH)_2$ crystals with uniform size when flow velocity vector in the reactor reaches a fixed value. Moreover, from the particle size distribution at

different line speed the relationship between relative particle size difference F (μm) and line speed V ($m \cdot s^{-1}$); $F_{(0.5-0.9)}=-15.59\ln V+41.172$ can be obtained.

(3) In the same retention time and chemical condition, from the XRD characterization it can be obtained that the relative crystallinity of $Ni(OH)_2$ crystals is proportional to the velocity distribution of the flow field size and uniformity in the reactor, and nickel hydroxide is proportional to the distribution range of the flow velocity vector and uniformity in the reactor. But the velocity distribution of the flow field size and uniformity in the reactor does not affect the crystallization of other crystal items. Moreover, the relationship between line speed V ($m \cdot s^{-1}$) and amorphization: $A=1-0.479\,4e^{0.104\,1V}$ can be obtained according XRD.

(4) The electrochemical activity of $Ni(OH)_2$ is proportional to the uniformity of flow distribution and velocity vector in the container when the residence time has no change. Moreover, it is confirmed that the electrochemical activity is proportional to the relative crystallinity and growth integrality of the spherical $Ni(OH)_2$.

References:

[1] PENG Mei-Xun(彭美勋), SHEN Xiang-Qian(沈湘黔), WANG Ling-Seng(王零森), et al. *J. Cent. South Univ. Technol.*(中南大学学报), **2005**,**12**(1):5-8

[2] Jiang L B, Zuo S B, Wang W J, et al. *J. Cryst. Growth*, **2011**, **318**(1):1089-1094

[3] Jaewon C, Seo S K, Cho G M, et al. *J. Mater. Res.*, **2012**,**27** (14):1-10

[4] Kile D E, Eberl D D, Hoch A R, et al. *Geochim. Cosmochim. Acta*, **2000**,**64**(17):2937-2950

[5] PENG Mei-Xun(彭美勋), SHEN Xiang-Qian(沈湘黔). *J. Cent. South Univ. Technol.*(中南大学学报), **2007**,**14**(3):310 -314

[6] Al-Hajry A, Umar A, Vaseem M, et al. *Superlattices Microstruct.*, **2008**,**44**(2):216-222

[7] Orikasa H, Karoji J, Matsui K, et al. *Dalton Trans.*, **2007**,**34**: 3757-3762

[8] Kühn M, Ehrenfried K, Bosbach J, et al. *Exp. Fluids*, **2012**, **53**(1):91-103

[9] Xia Q F, Zhong S. *Int. J. Heat Fluid Flow*, **2012**,**37**:64-73

[10]Zamankhan P. *Commun. Nonlinear Sci. Numer. Simul.*, **2010**, **15**(6):1511-1525

[11]Kosiwczuk W, Cessou A, Trinité M, Lecordier B. *Exp. Fluids*, 2005,39:895-908

[12]Sancho I, Varela S, Vernet A, et al. *Int. J. Heat Mass Transfer*, **2016**,**93**:155-166

[13]Fukushima C, Aanen L, Westerweel J. *Laser Techniques for Fluid Mechanics*. Berlin Heidelberg: Springer, **2002**:339-356

[14]Gandhi M S, Sathe M J, Joshi J B, et al. *Chem. Eng. Sci.*, **2011**,**66**(14):3152-3171

[15]Hua F, Olsen M J, Hill J C, et al. *Chem. Eng. Sci.*, **2010**,**65** (11):3372-3383